Theoretical and experimental studies of tunable ultraviolet–blue femtosecond pulses in a 405-nm pumped type I β-BaB_2O_4 noncollinear optical parametric amplifier and cascading sum-frequency generation

Chao-Kuei Lee

Photon-Factory, Institute of Electro-Optical Engineering, National Chiao Tung University, 300 Hsinchu, Taiwan, China

Jing-Yuan Zhang

Department of Physics, Georgia Southern University, Statesboro, Georgia 30460

J. Y. John Huang and Ci-Ling Pan

Photon-Factory, Institute of Electro-Optical Engineering, National Chiao Tung University, 300 Hsinchu, Taiwan, China

Received August 21, 2003; revised manuscript received January 11, 2004; accepted February 5, 2004

Femtosecond laser pulses that are tunable from 380 to 460 nm were directly generated from a 405-nm-pumped type I β-BaB_2O_4 noncollinear optical parametric amplifier (NOPA). A white-light supercontinuum from a CaF_2 plate excited by 810-nm pulses was seeded into the NOPA. A theoretical analysis showed that the near-UV-to-blue radiation generated is attributable to cascaded sum-frequency generation (SFG) of the output of the NOPA and the residual fundamental beam at 810 nm. One can tune the blue–UV light by either changing the orientation of the NOPA crystal or adjusting the angle between the pump and the seeding pulse. The optical conversion efficiency from the 405-nm pump to the tunable SFG radiation is more than 5%.

OCIS codes: 190.4410, 190.7110, 190.4970.

1. INTRODUCTION

Ultrafast optics is a rapidly evolving multidisciplinary field, and ultrafast pulses are widely used to excite materials and probe their subsequent evolution on ultrashort time scales.[1,2] Development of femtosecond laser sources with wide tuning ranges has yielded new research opportunities in femtochemistry and femtobiology.[3–5] Among the developments for generating femtosecond laser pulses with broad tunability, a particularly interesting trend is the combination of a high-intensity ultrashort solid-state laser with nonlinear optical frequency mixing.

A noncollinear optical parametric amplifier (NOPA) seeded with a white-light supercontinuum is attractive for its decreased pumping threshold and its ability reduce group-velocity mismatch (GVM) in ultrashort laser pulses. However, because of limitations of the phase-matching condition, the tuning range of a 400-nm-pumped type I β-BaB_2O_4 (BBO) NOPA is only 460–720 nm in the signal branch and 900 nm–2.4 μm in the idler branch. This limitation is unfortunate because tunable femtosecond pulses in the blue-to-near UV region (<460 nm) are useful in many applications that range from investigation of wide-bandgap materials to probing biomolecules. To extend the tuning range, one can use various nonlinear optical processes, such as sum-frequency generation (SFG) and second-harmonic generation (SHG), to convert the output of a NOPA to the desired short-wavelength radiation. Petrov *et al.* reported wavelength extension through cascaded second-order nonlinear frequency conversion.[6] However, the approach requires an additional SHG or SFG device for wavelength conversion. This complicates the entire tunable femtosecond laser system. Furthermore, a NOPA's SHG or SFG conversion efficiency is often limited.

Recently several groups of researchers demonstrated that femtosecond pulses near 400 nm can be generated with a deep-UV-pumped NOPA.[7–10] Using a 258-nm pump from a frequency-tripled femtosecond Ti:sapphire laser system, Tzankov *et al.* reported wavelength tuning from 346 to 453 nm.[11] These approaches to generating femtosecond deep-UV pulses are typically inefficient and require special deep-UV optics. Poor UV beam quality further aggravates the optical damage problem and limits conversion efficiency. We recently reported an alternative method of generating tunable femtosecond pulses from 380 to 465 nm near the degenerate point of a 405-

0740-3224/2004/081494-06$15.00

nm-pumped type I BBO NOPA.[12] We tentatively attributed this result to cascading SFG of optical parametric amplifier (OPA) pulses and the residual fundamental laser pulse at 810 nm in the same crystal for the NOPA. Tunable SFG output is readily available from the OPA stage without any additional frequency-conversion device. Although this UV–blue tuning range can also be obtained with direct SHG of an amplified Ti:sapphire laser with a tunable wavelength range of 760–920 nm, wavelength tuning of the amplified Ti:sapphire laser system is much more difficult than in our scheme reported here. Besides, its output wavelength cannot cover the full tuning range of a NOPA.

In Section 2 we present a theoretical analysis of this much simpler scheme for generating femtosecond tunable radiation. In Section 3 we describe and experimentally demonstrate the arrangement and performance of this approach. The tuning ranges for various seeding angles, the conversion efficiency, and the pulse profile are characterized in detail. With a pump energy of 75 μJ at 405 nm, the optical conversion efficiency from the pump to tunable SFG is more than 5%.

2. THEORETICAL ANALYSIS

Optical parametric amplification is part of the three-wave frequency mixing process. For efficient frequency conversion to be achieved, the laws of conservation of photon energies and momenta must be satisfied[14]:

$$\hbar\omega_p = \hbar\omega_s + \hbar\omega_i,$$
$$\hbar\mathbf{k}_p = \hbar\mathbf{k}_s + \hbar\mathbf{k}_i, \tag{1}$$

where ω_l and $\mathbf{k}_l$ denote frequency and wave vectors of the pump ($l = p$), signal ($l = s$), and idler ($l = i$) beams, respectively. Figure 1(a) illustrates the phase-matching scheme of the NOPA and the cascading SFG employed in our setup. To illustrate the distribution of the output beams about the pump direction, we show in Fig. 1(b) the beam configuration with a noncollinearly phase-matched BBO crystal.

The signal beam of a NOPA is injected into an appropriate nonlinear optical crystal with an angle α relative to the propagation direction of the pump beam. Here the sign of α is defined to be positive when the direction of the seeding signal beam is rotated counterclockwise from the pump beam. The idler beam is generated at an angle δ with respect to the signal beam. The cascading SFG satisfies the following law of conservation of energies and momenta:

$$\hbar\omega_{\mathrm{SFG}} = \hbar\omega_i + \hbar\omega_{810},$$
$$\hbar\mathbf{k}^{(e)}_{\mathrm{SFG}} = \hbar\mathbf{k}^{(o)}_i + \hbar\mathbf{k}^{(o)}_{810}, \tag{2}$$

where ω_{810}, $\mathbf{k}_{810}$, ω_{SFG}, and $\mathbf{k}_{\mathrm{SFG}}$ denote the frequency and wave vectors of the residual 810-nm pump beam and SFG, respectively. The resultant SFG is an e ray of a type I BBO NOPA and propagates at an angle δ' relative to the idler beam's direction:

$$\delta' = \tan^{-1}\left(\frac{|\mathbf{k}^{(o)}_{810}|\sin\delta}{|\mathbf{k}^{(o)}_{810}|\cos\delta + |\mathbf{k}^{(o)}_i|}\right),$$

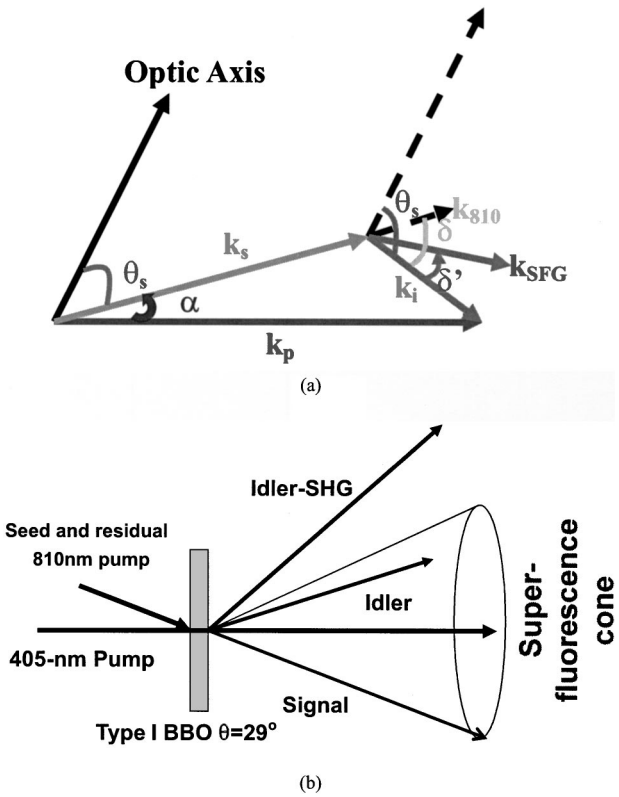

Fig. 1. (a) Schematic showing the noncollinear phase-matching conditions for an optical OPA and the cascading SFG of the OPA and a residual 810-nm pump beam. (b) Beam configuration in the noncollinearly phase-matched BBO crystal.

$$\delta = \theta_i - \theta_s, \tag{3}$$

where θ_s and θ_i are the angles of the signal and the idler, respectively, with respect to the optic axis.

Angle θ between the SFG beam and the optic axis can be calculated from

$$\theta = \theta_i - \delta'. \tag{4}$$

The index of refraction experienced by the SFG is

$$n^{(e)}_{\mathrm{SFG}} = \frac{n^{(o)}_{\mathrm{SFG}} n^{(e)}_{\mathrm{SFG}}}{\{[n^{(o)}_{\mathrm{SFG}}\sin\theta]^2[n^{(e)}_{\mathrm{SFG}}\cos\theta]^2\}^{1/2}}. \tag{5}$$

To depict properly the phase mismatching of three-wave mixing in the NOPA and in SFG, we express the summation of the wave vectors of optical pulses as

$$\Delta\mathbf{k} = \mathbf{k}_p - \mathbf{k}_s - \mathbf{k}_i,$$
$$\Delta\mathbf{k} = \mathbf{k}_{\mathrm{SFG}} - \mathbf{k}_{810} - \mathbf{k}_i. \tag{6}$$

With Eqs. (1)–(6) we can calculate the central wavelength and the tuning range of cascading SFG at various seeding angles by taking into account the phase-matching condition for the NOPA, SFG, and GVM among the optical pulses involved.

Figure 2 shows the calculated GVM between the residual pump beam of WLC at 810 nm and the idler beam of the NOPA along the direction of SFG with $\delta = -3°$. We found that the GVM becomes zero near 405 nm when the wavelength of the idler approaches the degenerate point and is smaller than 70 fs/mm as long as the SFG

wavelength lies at 350–450 nm. This result indicates that the pulse walk-off length of cascading SFG is sufficiently long to permit efficient SFG generation.

Figure 3 presents the tuning range of cascading SFG with various seeding angles α. Here, we determine the tuning range from a phase-matching tolerance that is equal to that at the FWHM bandwidth of the pulse spectrum. When the seeding angle ranged from $-3°$ to $-18°$, the phase-matching angle of the NOPA was found to overlap that for SFG in an ~400-nm-pumped type I BBO NOPA near its degenerate point of $\theta \sim 29°$. This result reveals that one can adjust the central wavelength of the cascading SFG from 410 to 440 nm by decreasing the seeding angle (Fig. 3, filled squares for $\Delta\mathbf{k} = 0$).

Tuning of the SFG output can be achieved in either of two ways: One is to change the seeding angle between the white-light supercontinuum (WLS) and the pump; the other is to scan the orientation of the crystal. As can be seen from Fig. 3, at larger seeding angles, such as $-15°$, where the central wavelength with $\Delta\mathbf{k} = 0$ is near 410 nm, small GVM and therefore large pulse walk-off length are found for wavelengths from 380 nm to ~460 nm. At a seeding angle of $\sim -8°$, the tuning range increases slightly to ~390 to ~500 nm. At an even smaller angle, such as $-2° \rightarrow -6°$, the tuning range breaks into two separate regimes. But, at such a smaller seeding angle, the GVM is large and the pulse walk-off length becomes shorter. We need to apply higher pumping intensity to generate stable SFG. In addition to this drawback, it is difficult to compensate for GVM from dispersion of the WLS by use of the NOPA. At a given seeding angle one can also tune the SFG wavelength by changing the orientation of the NOPA crystal; thus a continuous wavelength scan can be made.

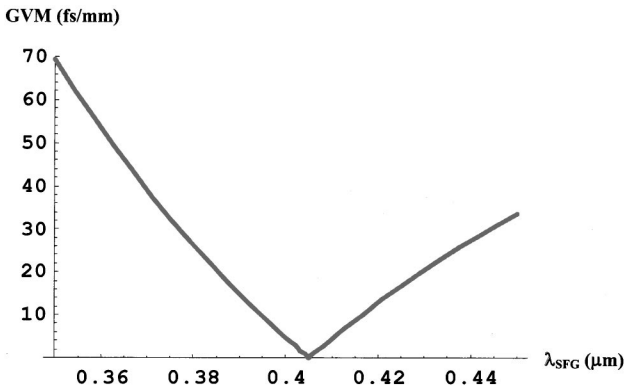

Fig. 2. Calculated GVM between the residual pump beam of WLC at 810 nm and the idler beam of a NOPA along the direction of SFG with $\delta = -3°$.

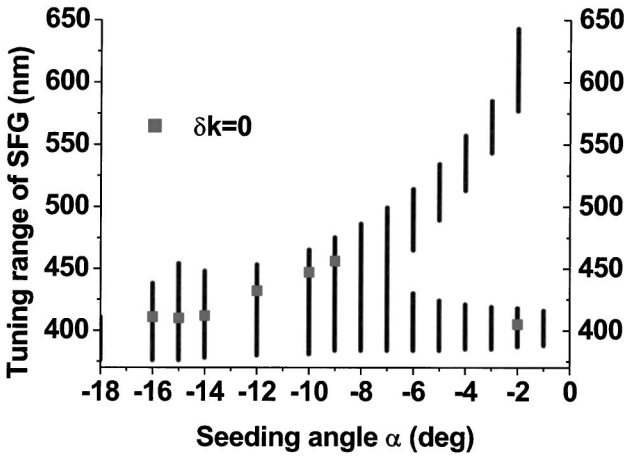

Fig. 3. Theoretical tuning curves of the cascading SFG at various seeding angles α between the OPA and the residual 810-nm laser beam in a 405-nm-pumped type I BBO NOPA.

3. EXPERIMENT

The experimental setup is shown in Fig. 4. An amplified femtosecond Ti:sapphire laser provides a pulse energy of 1 mJ at 810 nm with a pulse duration of ~90 fs and a 1-kHz pulse repetition rate. The output of the laser is split into two parts: 90% of the energy is frequency doubled to 405 nm with 0.3-mm-thick BBO for pumping the NOPA. The frequency-doubling pulse energy is adjustable from 50 to 120 μJ with a pulse duration of ~60 fs. The other 10% of the Ti:sapphire laser beam is used to generate a WLS with a 2-mm-thick CaF_2 plate. The CaF_2 plate is employed to reduce chirping in the WLS and to increase the seeding intensity such that the OPA pulses can be stronger and more stable. The WLS overlaps temporally and spatially the 405-nm pump beam in 2-mm-thick type I BBO cut at $\theta = 29°$. The pump intensity of the NOPA BBO crystal is $5-12 \times 10^{13}$ W/cm^2. Beam-crossing angle α between the seeding and the pump pulses is adjustable from $-2°$ to $-18°$.

About the degenerate point of the NOPA a bright beam with a wavelength that is tunable from the near UV to the blue can readily be observed. The inset of Fig. 4 shows the output of the NOPA projected onto a white paper. The ring is the parametric superfluorescence, and the black spot at the center of the ring indicates the position of the residual pump beam at 405 nm. We punched a hole in the screen to let the residual pump beam pass through the hole to prevent saturation of the CCD camera by the scattered residual pump beam. The red spot on the right-hand side of the pump and near the superfluorescence ring is the output of the OPA. On the left-hand side of the pump the spot outside the ring originates from the tunable SHG of the OPA component, and the bright spot inside the ring is widely tunable from 380 to 460 nm.

We found experimentally that the bright and widely tunable spot in the UV–blue spectrum can be attributed to SFG from the NOPA and the residual pump beam at 810 nm that is used in WLS generation. At a seeding angle of $-14°$, SFG was observable even below the pumping threshold of parametric superfluorescence. However, when the seeding angle was decreased to $-6° \rightarrow -8°$ we had to pump the NOPA crystal to a level at which bright and stable parametric superfluorescence was obtained. Further reducing the seeding angle made SFG difficult.

Based on the calculation of the GVM among SFG, OPA, and 810-nm pulses, we found that a seeding angle of $-8.4°$ to $-14°$ is most appropriate for cascading SFG. At a small seeding angle of $\sim -1.5°$, the large GVM leads to a short pulse walk-off length in the crystal and therefore weakens the cascading SFG. Note that at the small seeding angle we can still observe several blue spots, which could be attributed to SHG of the OPA and cascad-

ing SFG. As shown in Fig. 5, at a small seeding angle of $\sim -2°$ the phase-matching curve of the cascading SFG crosses that of the SHG of the idler at a wavelength near 800 nm. Therefore it is possible to simultaneously observe SHG of the NOPA idler wave and cascading SFG at a small seeding angle. Although SHG of the NOPA allows the wavelength to be extended to 380 nm or lower, its output energy is significantly lower than the cascading SFG at a large seeding angle. Baltuska *et al.* also reported direct SHG of an idler from a NOPA, which they used to interfere with the signal wave to monitor the carrier-envelope slip.[13] However, direct generation of cascading SFG from a NOPA has not yet been demonstrated and characterized.

We can adjust the central wavelength of the cascading SFG by varying the orientation of the NOPA crystal with a given seeding angle. As shown in Fig. 6(a), with a seeding angle of $-14°$ the tuning range is 395 to 465 nm; similarly, with a seeding angle of $-8.4°$ the tuning range can extend from 380 to 432 nm (not shown here). Figure 6(b) shows the pulse energy of SFG output at various wavelengths for a pump energy of 120 μJ at 405 nm. The energy fluctuation of the SFG output was found to be less than 5%. Figure 7 shows the theoretical tuning range and the SFG wavelength with $\Delta\mathbf{k} = 0$ for a variety of seeding angles α. The measured wavelengths with $\alpha = -8.4°, -14°$ are also included for comparison. We found that the experimental results (open symbols) agree well with the theoretical calculation (solid lines). The measured SFG wavelength with maximum gain (the star symbols) also coincides well with the calculated phase-matched SFG wavelength with $\Delta\mathbf{k} = 0$ (the filled squares). These results firmly support our concept of the origin of the tunable UV–blue radiation from a NOPA.

Cascading SFG yields a fairly high optical conversion efficiency. For example, with a pump energy of 75 μJ/pulse at 405 nm the pulse energy of the SFG output at 444 nm was measured to be ~ 4 μJ, which corresponds to an optical conversion efficiency of more than 5% from the pump to SFG. One can increase the output of SFG by increasing the total energy used for WLS generation; thus

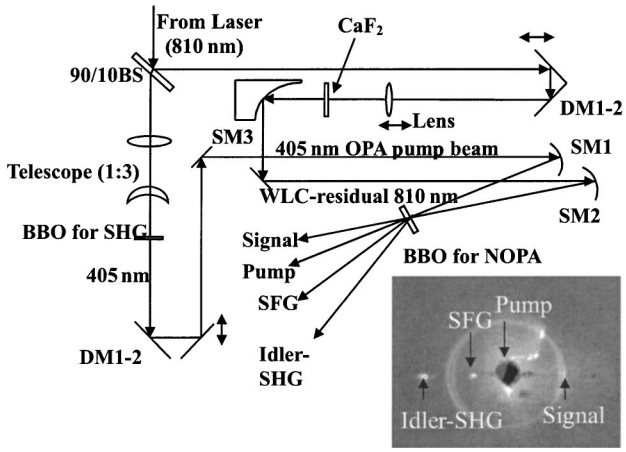

Fig. 4. Experimental setup of the NOPA and the cascading SFG employed in this study: DM-1, DM-2, dielectric mirrors; SM1–SM3, spherical mirrors. Inset, beam pattern of the NOPA output projected onto a white screen. The image was taken with a seeding angle of $-8°$.

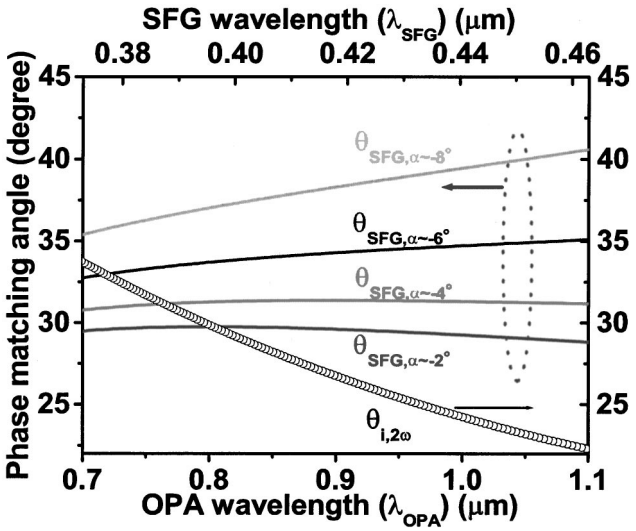

Fig. 5. Calculated curves of the phase-matching angle of the cascading SFG (left-hand y axis) and the SHG of a NOPA idler wave (right-hand y axis) as a function of the optical wavelength of an OPA (x axis, bottom) and of a SFG (x axis, top).

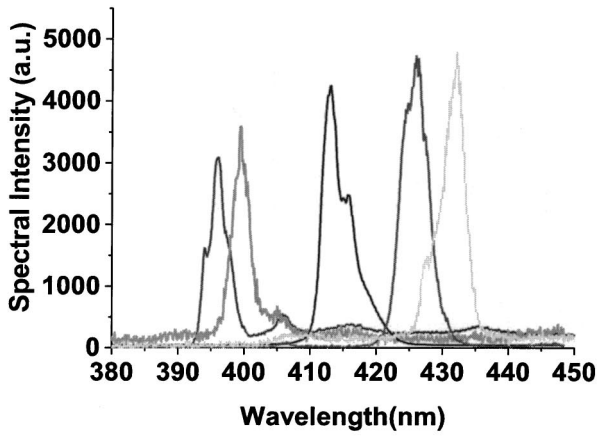

(a)

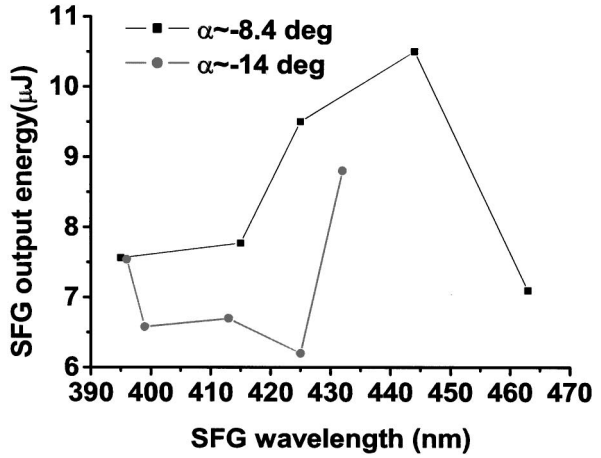

(b)

Fig. 6. (a) Spectrum of the cascading SFG with various orientations of BBO at seeding angle $\alpha \sim -14°$. (b) Pulse energies of SFG output at various wavelengths with a pump energy of 120 μJ at 405 nm.

the residual radiation at 810 nm is higher. Figure 8 presents a plot of the SFG output energy at 444 nm with a variety of residual pulse energies at 810 nm, which is along the WLS seeding beam. The observed linear dependence of SFG output power on the residual 810-nm beam provides extra supporting data for our notion of the mechanism for cascading SFG.

As noted above, we can also produce tunable near-UV–visible femtosecond pulses by frequency doubling the output of the OPA or use SFG to combine the output of an OPA with the fundamental laser at ~810 nm. However, these schemes require an extra nonlinear optical crystal and require synchronous tuning of at least two crystals, making the operation of these devices complicated.

By using the newly developed OPA-based frequency-resolved optical gating[15] (FROG) we can fully characterize the output of the NOPA. Figure 9 shows the measured OPA FROG trace and its retrieved amplitude and phase of the NOPA component at 571 nm. The retrieved OPA FROG trace shows that no significant chirping in the NOPA output pulse. The pulse duration of the NOPA is ~75 fs. We also employed a single-shot XFROG[16] to deduce the pulse profile of the cascading SFG and found a

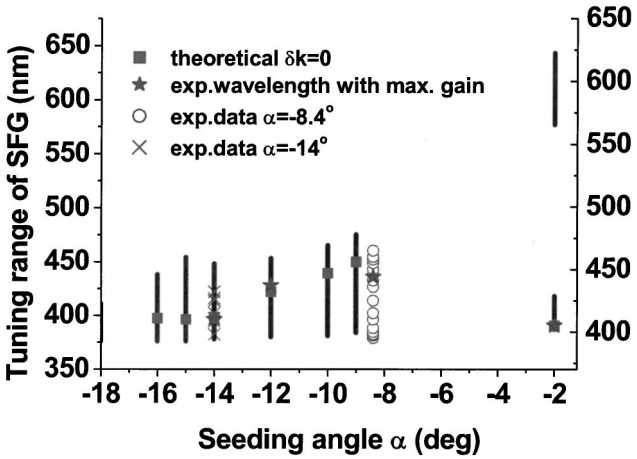

Fig. 7. Theoretical tuning range and the cascading SFG wavelength with maximum gain for various values of α. Experimental data for SFG wavelengths with seeding angles of $-8.4°$ and $-14°$ are included for comparison.

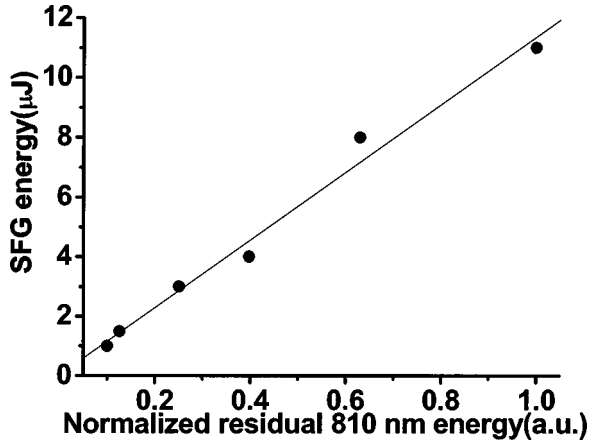

Fig. 8. Output power of the cascading SFG at 444 nm as a function of the average power of the residual 810-nm pump beam.

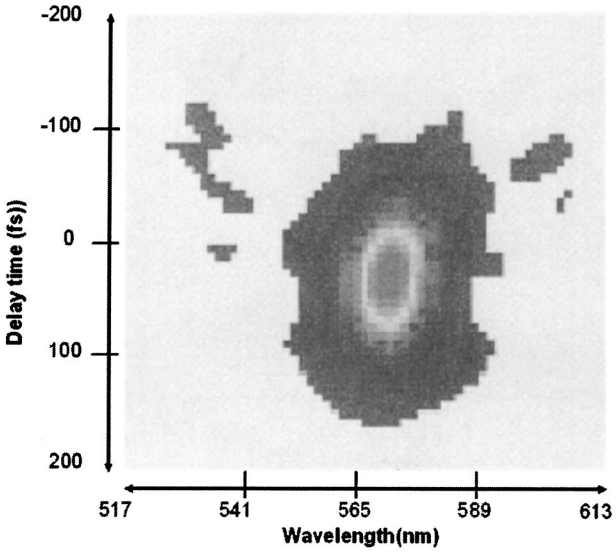

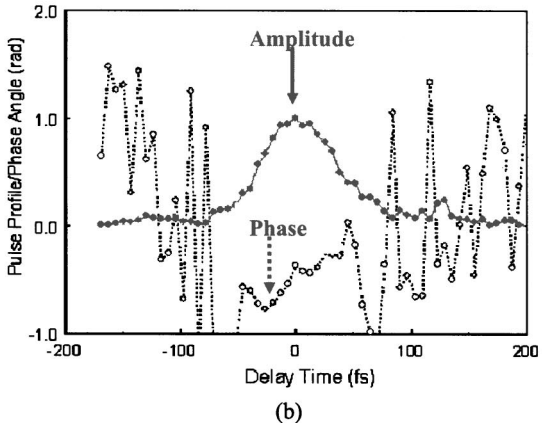

Fig. 9. (a) Measured OPA FROG trace of the NOPA output at 571 nm. (b) Retrieved pulse profile (solid curve) and phase of the NOPA output.

FWHM duration of ~100 fs. The value is greater than that of the corresponding NOPA but less than that of the residual 810-nm pulse. The longer pulse duration can be attributed to the larger GVD at shorter wavelength in BBO. This result also agrees with the notion that the SFG component is a temporal convolution of the NOPA component and the residual fundamental beam. The OPA component is generally shorter than that of its pump at 405 nm, which is shorter than its fundamental pulse at 810 nm.

4. SUMMARY

In conclusion, we have successfully demonstrated the generation of femtosecond laser pulses tunable from 380 to 460 nm by cascading sum-frequency generation in a 405-nm-pumped type I noncollinearly phase-matched optical parametric amplifier. Furthermore, we theoretically analyzed this much simpler scheme for generating femtosecond tunable radiation. Tuning ranges at various seeding angles, conversion efficiencies, and pulse profiles have been characterized in detail. The energy conver-

sion efficiency of the SFG is more than 5%. The reported scheme provides a simple and effective way to extend the tuning range of a 405-nm-pumped type I β-BaB_2O_4 NOPA from 460 to 380 nm without the need for any additional frequency-upconversion stage. It was also found that the beam quality and the pulse shape of the SFG component are approximately the same as those of the OPA.

ACKNOWLEDGMENTS

The authors acknowledge sponsorship by the National Science Council under various grants and by the Pursuit of Academic Excellence Program of the Ministry of Education, Republic of China. J.-Y. Zhang is grateful for the support of Georgia Southern University during his sabbatical.

C.-K. Lee's e-mail address is chuckcklee@yahoo.com.

REFERENCES

1. For an overview of the state of the art of ultrafast spectroscopy, see, for example, T. Elsaesser, S. Mukamel, M. M. Murnane, and N. F. Scherer, eds., *Ultrafast Phenomena XII*, Vol. 66 of Springer Verlag Series in Chemical Physics (Springer-Verlag, Berlin, 2001).
2. T. Brabec and F. Krausz, "Intense few-cycle laser fields: frontiers of nonlinear optics," Rev. Mod. Phys. **72**, 545–591 (2000).
3. A. H. Zewail, "Femtochemistry: atomic-scale dynamics of the chemical bond," J. Phys. Chem. **104**, 5660–5694 (2000).
4. N. H. Damrauer, G. Cerullo, A. Yeh, T. R. Boussie, C. V. Shank, and J. K. McCusker, "Femtosecond dynamics of excited-state evolution in $[Ru(bpy)_3]^{2+}$," Science **275**, 54–57 (1997).
5. T. Elsaesser, S. Mukamel, M. Murnane, and N. F. Scherer, "Ultrafast phenomena XII," in *Proceedings of the 12th International Conference* (Springer-Verlag, New York, 2000).
6. V. Petrov, F. Seifer, O. Kittelmann, J. Ringling, and F. Noack, "Extension of the tuning range of a femtosecond Ti-:sapphire laser-amplifier through cascaded 2nd-order nonlinear frequency-conversion," J. Appl. Phys. **76**, 7704–7712 (1994).
7. K. Osvay, G. Kurdi, J. Klebniczki, M. Csatari, and I. N. Ross, "Demonstration of high gain amplification of femtosecond ultraviolet laser pulses," Appl. Phys. Lett. **80**, 1704–1706 (2002).
8. K. Osvay, G. Kurdi, J. Klebniczki, M. Csatari, I. N. Ross, E. J. Divall, C. H. J. Hooker, and A. J. Langley, "Broadband amplification of ultraviolet laser pulses," Appl. Phys. B **74**, S163–S169 (2002).
9. K. Osvay, G. Kurdi, J. Klebniczki, M. Csatari, I. N. Ross, E. J. Divall, C. H. J. Hooker, and A. J. Langley, "Noncollinear optical parametric amplification of femtosecond UV pulses," presented at the Conference on Lasers and Electro-optics, Munich, Germany, June 18–22, 2001.
10. P. Tzankov, T. Fiebig, and I. Buchvarov, "Tunable femtosecond pulses in the near-ultraviolet from ultrabroadband parametric amplification," Appl. Phys. Lett. **82**, 517–519 (2003).
11. P. Tzankov, I. Buchvarov, and T. Fiebig, "Broadband optical parametric amplification in the near UV–vis," Opt. Commun. **203**, 107–113 (2002).
12. C.-K. Lee, J.-Y. Zhang, J. Y. Huang, and C.-L. Pan, "Generation of femtosecond laser pulses tunable from 380 nm to 465 nm via cascaded nonlinear optical mixing in a noncollinear optical parametric amplifier with a type-I phase matched BBO crystal," Opt. Express **11**, 1702–1708 (2003), http://www.opticsexpress.org.
13. A. Baltuska, T. Fuji, and T. Kobayashi, "Self-referencing of the carrier-envelope slip in a 6-fs visible parametric amplifier," Opt. Lett. **27**, 1241–1243 (2002).
14. Y. R. Shen, *Principals of Nonlinear Optics* (Wiley, New York, 1984).
15. J. Y. Zhang, A. P. Shreenath, M. Kimmel, E. Zeek, R. Trebino, and S. Link, "Measurement of the intensity and phase of attojoule femtosecond light pulses using optical-parametric-amplification cross-correlation frequency-resolved optical gating," Opt. Express **11**, 601–609 (2003), http://www.opticsexpress.org.
16. J.-Y. Zhang, C.-K. Lee, J.-Y. J. Huang, and C.-L. Pan, "Sub femto-joule sensitive single-shot OPA-XFROG and its application in study of white-light supercontinuum generation," Opt. Express **12**, 574–581 (2004).